Jurnal
Teknologi

Full Paper

THE DEVELOPMENT OF A MULTI-PURPOSE WIND TUNNEL

Zambri Harun[a,b,*], Wan Aizon W. Ghopa[a,b], Shahrir Abdullah[a,b], M. Izhar Ghazali[a], Ashraf Amer Abbas[a], Mohd Rasidi Rasani[a,b], Rozli Zulkifli[a,b], Wan Mohd Faizal Wan Mahmood[a,b], Mohd Radzi Abu Mansor[a,b], Zulkhairi Zainol Abidin[a,b], Wan Hanna Melini Wan Mohtar[a]

[a]Faculty of Engineering and Built Environment, Universiti Kebangsaan Malaysia, 43600 UKM Bangi, Selangor, Malaysia
[b]Centre for Automotive Research, Faculty of Engineering and Built Environment, Universiti Kebangsaan Malaysia, 43600 UKM Bangi, Selangor, Malaysia

Article history
Received
18 December 2015
Received in revised form
10 March 2016
Accepted
25 April 2016

*Corresponding author
zambri@ukm.edu.my

Graphical abstract

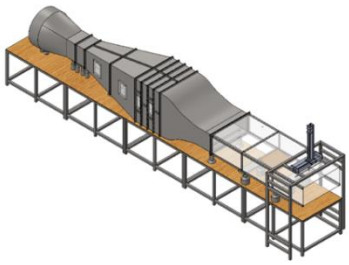

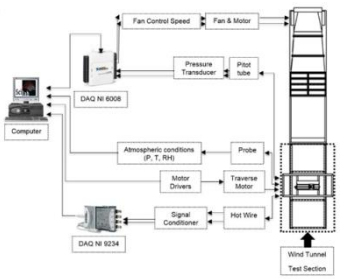

Abstract

This manuscript contains the development stages of a multi-purpose wind tunnel built at the Faculty of Engineering and Built Environment, Universiti Kebangsaan Malaysia. The fully automated wind tunnel is named Pangkor after an island in Perak, Malaysia. The development of the wind tunnel consists of three stages namely the design, fabrication and testing & commissioning. The computational fluids dynamic (CFD) approach was employed to ascertain the main geometries to optimize space utilization. Calculations are made based on typical wind tunnel design guidelines. Pitot tubes-pressure transducer, hotwire anemometry, temperature, room humidity and barometric sensors were used to verify actual flow of our construction. A traverse installed at the wind tunnel is capable of a two dimensional movements. The 15 kW axial fan used is especially selected because of space limitation. A variable frequency drive (VFD) connected to fan's motor allows velocity control from a computer. All devices are connected a computer with one single controlling software; Scilab – ensuring ease of operation. The project shows that, with a limited budget, a wind tunnel with full functionalities could be constructed.

Keywords: Wind tunnel; boundary layer

Abstrak

Manuskrip ini mengandungi dokumentasi peringkat-peringkat pembangunan sebuah cerowong angin pelbagai guna yang dibina di Fakulti Kejuruteraan dan Alam Bina, Universiti Kebangsaan Malaysia. Cerowong angin automatik sepenuhnya ini dinamakan Pangkor, iaitu nama sebuah pulau di Perak, Malaysia. Terdapat tiga bahagian utama di dalam pembangunan cerowong angin ini iaitu reka bentuk, pembinaan dan pengujian & pentauliahan. Kaedah dinamik bendalir komputeran digunakan untuk memastikan geometri utama dan pengoptimuman penggunaan ruang. Pengiraan dibuat berdasarkan garis panduan pembinaan cerowong angin. Tiub Pitot-transduser tekanan, anemometri dawai panas, penderia-penderia suhu, kelembapan bilik, jangka-tekanan (barometer) digunakan untuk memastikan aliran angin sebenar pembinaan ini. Sebuah terabas (traverse) dipasang di cerowong angin boleh digunakan untuk pergerakan dua dimensi. Kipas paksi 15 kW digunakan atas faktor keluasan yang terhad. Pacuan frekuensi bolehubah (VFD) bersambung kepada kipas membolehkan kawalan kelajuan angin dibuat dari komputer. Semua peranti bersambung kepada sebuah komputer dengan satu perisian untuk pengawalan; Scilab – memastikan operasi yang senang. Projek ini menunjukkan walaupun dengan kedudukan dana yang rendah, sebuah cerowong angin dengan fungsi menyeluruh boleh dibina.

Kata kunci: Cerowong angin; lapisan layer

1.0 INTRODUCTION

Wind tunnels are widely used to measure aerodynamic behaviour of solid objects. These facilities provide actual drags, lift and other aerodynamic properties important for aircraft operations, car aerodynamic features such as side mirror, bicycle helmet and etc. Having wind tunnel facilities was considered of strategic importance during the Cold War; the development of supersonic aircraft as well as missiles gave upper hands advantages in the war. Early studies of wind tunnel were recorded in 1742 and 1759, simulated by Robins [1] and Smeaton [2], where both studies used rotational object on an arm to create the air flow. Wind tunnel are widely used to study aerodynamic properties of flow past an object/s e.g. in the automotive industries [3] or simply flow properties on the wall i.e. boundary layer studies [4].

Wind tunnel experiments also provide the necessary information for much larger atmospheric-scale boundary layer studies. The wind tunnels results are compared with bigger facilities for especially flow similarities [4], [5]. The features of natural wind in the atmospheric boundary layer were only properly simulated in 1950s [6], [8]. Since then, extensive research have been conducted to improve the wind characteristics in the wind tunnel, notably by placing flow-adjustment devices and the advancements in data-acquisition systems [9], [10]. Wind tunnel permits an exploration of atmospheric boundary layer effects on building structures, pollutant dispersion, wind-induced vibration and weather prediction [11], [15]. Investigation of simulated natural wind characteristics on small-scale models in boundary-layer wind tunnel (BLWT) contributed to enhancement of scope and accuracy in both research and design.

Even with recent and updated technologies, materialising a functional wind tunnel proved to be a challenge, particularly with restricted funding. This artcile describes the development of low-cost, multi-purpose and automated close-circuit wind tunnel. The paramount requirement is to have a proper simulation of the characteristics of a controlled flow using local material, in-house fabrication and self-assembly. Even working with limitations, attentions were paid to the foregoing requirements of surface roughness, flow structure, pressure gradient and sufficient upwind fetch.

2.0 DESIGN

2.1 Planning

Prior to starting detailed design works, the team deliberated a few main criteria which were (a) the type of wind tunnel to be constructed, (b) available funds, (c) space in laboratory and (d) benchmarks. The first three items are inter-related; the wind tunnel designs should be tailored to meet the specific research goal and is subject to budget and facility limitations. We decided that the wind tunnel should be used to study the flow characteristics/aerodynamic of objects, boundary layer as well as for the use of particle image velocimetry (PIV). With the space available at Makmal Kejuruteraan Air dan Pantai (The Laboratory of Water and Beach Engineering), Department of Civil and Structure, Faculty of Engineering and Built Environment, UKM, a space of about 12 m long, 4 m wide and 3 m height allows for the use of wind tunnel facility. The place was only use for laboratory works either for undergraduates or for research works. Noise, vibrations and potential hazards from the operations of a wind tunnel will unlikely affect existing use of the laboratory which currently holds typical undergraduate laboratory works.

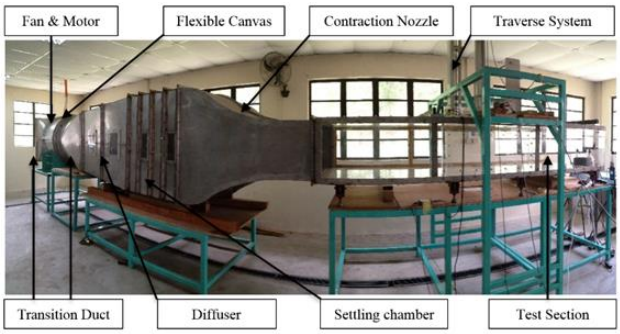

(a) Snap-shot

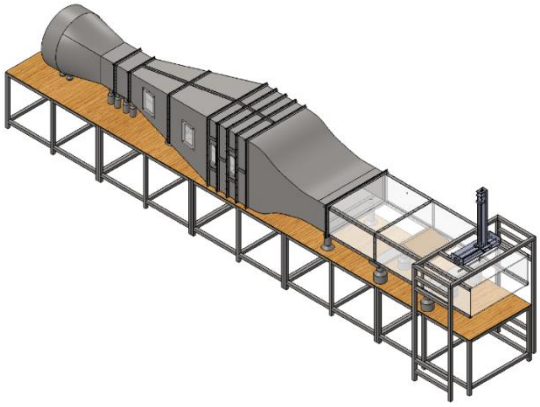

(b) Perspective drawing

Figure 1 General view of the wind tunnel at Makmal Kejuruteraan Air dan Pantai, Faculty of Engineering and Built Environment, UKM. (a) A snapshot taken during wind speed calibration of devices belonging to research related to architectural design and (b) perspective drawing of the wind tunnel

The facility has existing typical mechanical services such as ventilation and plumbing & sanitary and electrical services such as lighting and more importantly an electrical source for the fan and motor. Furthermore, a *wifi* connection is within good range and this is important for detecting faults in the programming required to automate the wind tunnel. At the start, funds were low and only main equipment were purchased/constructed such as the settling chamber, contraction section and the stands.

The team made a few visits to local institutions where wind tunnel facilities were available [16], [17] in 2013. From these visits, general requirements such as the needs of hotwire etching chamber (hotwire is the sensor for hotwire anemometry), programmable traverse, and automatic operations of wind tunnels for ease of measurement were taken into considerations.

2.2 Main Design Criteria

The general layout of the open circuit wind tunnel is shown in Figure 1. The wind tunnel consists of a transition duct, blower, diffuser, settling chamber, and contraction nozzle and test section at the end of the duct. A 2-axis travel can be seen located above the test section.

Fan motor. The brand of fan motor is Elprom with 15 kW controlled by a variable frequency drive (VFD). We have chosen an axial fan model MSA 1000 because of the space limitation, fan capacity and efficiency. This fan is comparatively small and can fit in the laboratory.

Transition Duct/ Conversion Duct. The cylindrical duct has been used to allow the installation of the axial flow fan which works as drive system for the upstream flow. Thus, the transition duct with conical shape (D = 1000 mm) at just at the exit of the motor section converts the flow from rectangular to conical shape (W x D = 1000 mm x 1000 mm). To ensure that no harmful flow occurs while passing this duct, numerical study has been performed and the flow characteristics confirmed before proceeding with the rest of design. The total length of conversion duct is approximately 1.5 m.

Diffuser. The diffuser is located just downstream of the conversion duct. The cross sectional area of diffuser increases mildly to avoid separation of flow. Therefore, the settling chamber will have to take on the exit side of diffuser. A diffuser reduces the fluid kinetic energy while increasing the static pressure inside the duct. It decelerates the high-speed flow from the blower side. The flow through a diffuser depends on its geometry defined by the area ratio, diffuser angle, wall contour and diffuser cross-sectional shapes. The required diffuser to design is with minimum level of flow separation. Present design diffuser duct is based on experimental results by Kline's experiments [18] who studied the two dimensional flow inside the diffuser under the effect of diffuser angle and their length, as shown in Figure 2. We also considered newer design parameters performed by the group at the Royal Institute of Technology (KTH) [19].

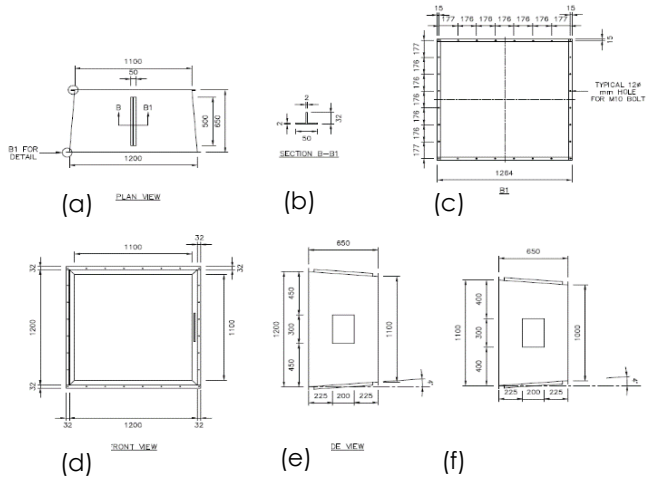

Figure 2 Diffuser details. (a-e) detail which connects the wider section of the diffuser to the settling chamber, (f) the narrower section of the diffuser

The plan views of the diffuser are shown on Figure 2(a) and 2(f), The total length of diffuser, 1300 mm and the heights at inlet of 1000 mm and at the outlet of 1200 mm produces mild increase of flow area i.e. diffuser angle of θ = 4.4°. Refer to Figure 3(a) to calculate θ. From Figure 3(a) also, the ratio of flow length X and flow width W_i could be determined i.e. X/W_i = 1.3. The X : W_i ratio suggests that the design to be in the region A i.e. a stable flow. The diffuser angle here is well above the requirement to avoid separation and within the recommendation of θ = 5° to 7° [20].

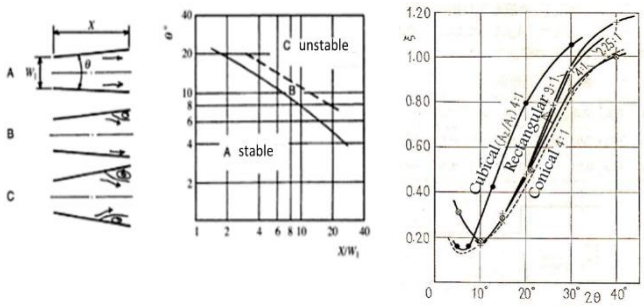

(a) Kline's experiment 's guideline [18] - two dimensional flow inside diffuser

(b) The Gibson's method [21] - loss coefficient at various diffuser angles

Figure 3 Guidelines to diffuser design from Kline's experiment and from the Gibson's method

The Gibson's method, as in Figure 3(b), provides a guideline for pressure loss estimation in the diffuser [21], [23]. Figure 3(b) illustrates three different shapes of diffuser duct; cubical, rectangular and conical. All cases mentioned above show loss coefficient which increases with diffuser angles. The present diffuser duct has an entrance area of 1000 mm x 1000 mm and exit area of 1200 mm x 1200 mm. That represents cubical ratio *A2/A1* of 1.44. The equivalent pressure loss coefficient is in between 0.2 to 0.3.

The loss coefficient through the screen needs to be considered. Here, the details study of screen inside the diffuser section presented by Mehta and Bradshaw [22] is repeated. Two layers of screen are installed at the beginning and between the two-part diffuser sections. Each screen with two-layer 15 mm and 4 mm wire mesh have been used to improve the flow quality by controlling or curbing the boundary layer separation [28]. Screens are also used to reduce the turbulence intensity [32]. The details study of screen inside the diffuser section is presented by Mehta and Bradshaw [22]. The formulation for predicting pressure drop coefficient *K* through the screen proposed by Wieghardt [29], is used here;

$$K = 6.5\left[\frac{1-\beta}{\beta^2}\right]\left[\frac{Ud}{\beta\nu}\right]^{-0.33} \quad (1)$$

All factors affecting the pressure loss coefficient are calculated, the screen open-area ratio $\beta = (1 - d/l)^2$, and it is recommended that $\beta < 0.5$ [28], here *d* is the screen wire diameter, *l* is the screen mesh length and v is the kinematic viscousity. It is found that the range of velocity for the application is $0 < U < 20$ m/s as suggested by [30], [31]. Table 1 shows the details of screen calculation by applying Eq. 1.

Table 1 Details of screen

Screen	Wire diameter *d* (mm)	Mesh length *l* (mm)	Open – area ratio *β*	Pressure loss coefficient *K* at *U* = 10 m/s
1st layer	1	15	0.87111	0.1261
2nd layer	0.5	4	0.7656	0.3575

The turbulence intensities reduction can be obtained by applying the ratio $1/\sqrt{1+K}$ [32]. Applying this ratio produces 0.9423 and 0.8583 generated by the two layer of screens respectively. This results in a composite turbulence intensity reduction factor of 0.654 due to the two screens (the two values multiplied for the smaller and bigger mesh and then squared to reflect that two part of screens of the same screen geometries have been used). The turbulence intensity reduction due to the contraction by using Batchelor's relation [33], [34] with contraction ratio 2.4 can be obtained by the following equation,

$$u' = \frac{1}{2c}\left[3\left(\ln 4c^3 - 1\right)\right]^{1/2} \quad (2)$$

Where *c* is the contraction ratio. The result is a reduction factor of 0.692 due to the contraction alone. Hence, the composite turbulence reduction factor for the combined screens and contraction is 0.452 and by assuming the inlet turbulence 10%, the total turbulence intensity by screens and contraction nozzle is to be on the order of 0.045 or 4%.

Settling Chamber

In most tunnels, the flow conditioning section contains a honeycomb, screens and a settling chamber. Once the flow exits the diffuser section, it passes the settling chamber (see Figure 1). The uniformization process starts in the settling chamber. In the case of low quality flow requirement, a simple constant section duct could be provided to connect the settling chamber exit to the entrance of the contraction nozzle. However, when a high quality flow is required, some devices can be installed to increase flow uniformity and reduce the turbulence levels at the entrance of contraction. The most commonly used devices are screen and honeycombs. Note again that the installation of these devices could contribute to the pressure loss [22].

Contraction Nozzle

The inlet contraction plays a critical role in determining the flow quality in the test section. A well designed contraction nozzle should speed up the flow, decrease turbulence intensity and create a uniform flow, while avoiding separation before entering the test section. Based on Figure 4(a), the contraction nozzle need to be axisymmetric shape and more than 15 different methods have been proposed, and few have been experimentally tested [24]. Present design

of two-dimensional contraction nozzle is the same method proposed by Rouse and Hassan [25], which was based on electrical field analogy to obtain the axisymmetric line. A schematic of the contraction shape polynomials is explained by Figure 4(b) and Eq. 3 and 4.

$For\ 0 \le x \le x_i$

$$\frac{R}{D/2} = \frac{D_s}{D} - \left(\frac{D_s}{D} - 1\right)\frac{(x/L)^3}{(x_i/L)^2} \quad (3)$$

$For\ x_i \le x \le L$

$$\frac{R}{D/2} = 1 + \left(\frac{D_s}{D} - 1\right)\frac{(1-x/L)^3}{(1-x_i/L)^2} \quad (4)$$

Here, distance from centreline to measured contraction wall is *R*, the distance in streamline direction is x, entrance contraction diameter is D_s, exit contraction diameter is *D*, contraction nozzle length is *L* and the two polynomials are matched at a specified location x_i. Due to the demand of wider test section area for the present work, the contraction ratio is limited to 2.4:1 with total length of 1400 mm. Figure 4(b) illustrates the polynomials shape obtained from the calculation based on this method. Note that, the matched point of polynomials shape occurs at x = 375 mm.

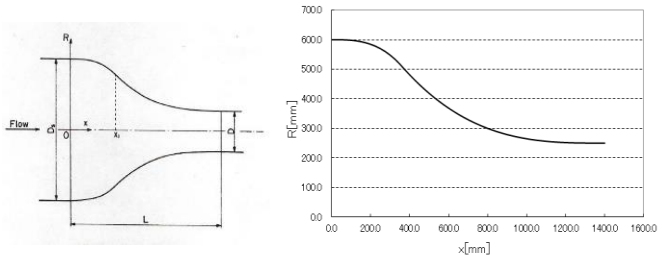

(a) Guideline for contraction [24] (b) Calculated contraction for current design

Figure 4 The design approach for the contraction nozzle

Test Section. The test section is made from 15 mm thick acrylic sheets. Transparent test section is preferred for its ease of operation. The test section has 1200 mm width, 500 mm and 2000 mm long. The frame is made from stainless steel 'L' bars. Since it is possible that some of the sections sag, the top part of the test section are sufficiently connected with ball screws so that test section upper section's desired levels could be achieved. A constructed traverse is placed on the test section as shown in Figure 1(a) and 1(b). Maximum speeds possible with the current settings is 25 m/s.

Traversing Mechanism And Rotating Table

2-Axis Traverse and Rotating Table. Figure 5(a) shows a 2-axis traverse. The purpose of the traverse system is for mounting sensors namely the Pitot tube, hotwire or temperature probes. The 2-axis mechanism is composed of two sliders in two-set guides (vertical and horizontal). This traverse is powered by two fine-step, stepper motors (400 steps per revolution). The traverse is built taking largely the design from the University of Melbourne's Green Tunnel 2-axis traverse construction [26].

The Vecta steppers motors model PK266-034 are connected to motor Velmex controllers with model VXM-3. With ball screw pitch of 1.6 mm for both vertical and horizontal, the traverse gives a movement finer than 0.1 mm, or 4 x 10^{-3} mm per step to be exact.

Figure 5(b) shows the rotating table. The material for the main support structure is 50 mm x 50 mm hollow mild steel with 4 mm thickness. The protractor is made from aluminum block of 10 mm thickness. The engraving of the protractor was implemented using CNC machine. The main rod that will reach into the middle section of the wind tunnel's test section is made from 16 mm stainless steel rod. The 16 mm diameter rod was previously used by this group in the NACA 0026 test at Universiti Teknologi Malaysia, skudai and it appeared that this size sufficiently held our 600 mm span x 615 mm chord x 15.6 mm thickness NACA 0026 airfoil firmly and without significant vibrations [27].

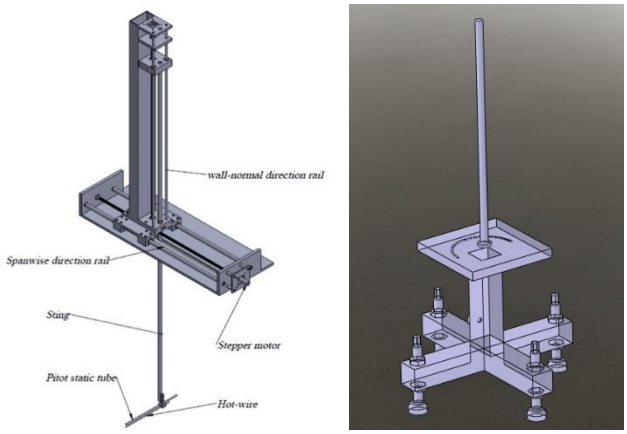

(a) 2-axis traverse (b) Rotating table

Figure 5 (a) 2-axis traverse based on the University of Melbourne traverse [26] and (b) a rotating table based on UTM's low speed wind tunnel (LSWT) [16]

2.3 Automation

The most important features of the wind tunnel is its functionalities and ease of use. As mentioned before, a single point control is preferred because operations can be made simple. Scilab is the only software used for controlling air flow speeds, traverse system and the acquisition operations.

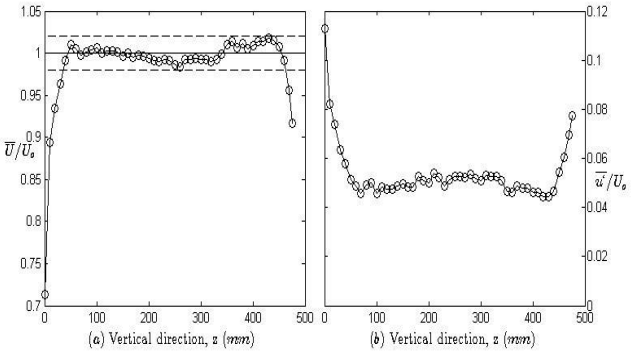

Figure 6 Diagram of connectivity of all devices to a computer using Scilab

Figure 6 shows the diagram of all connectivity. Starting from the motor, a National Instrument (NI) data acquisition (DAQ) system is used to send signal to the VFD. The fan speed was controlled through an output voltage signal produced by the NI DAQ 6008 module under request of Scilab. The rest of connectivity for all sensors, stepper motors and other devices are listed in the diagram. We have to leave the details and readers are encouraged to visit www.ukm.my/zambri/consult/WT.htm for Scilab programming codes and the connection methods.

3.0 FLOW QUALITY AND COMMISSIONING

Prior to hotwire and pitot tube measurements, the wind tunnel has been run continuously for eight hours for different fan frequency to test fan general working performance including speeds and temperature. No abnormalities were observed except for insufficiency current.

Flow qualities are the only analysis presented here. Figure 7(a) shows the velocity profile at the centerline of the wind tunnel, 1700 mm from the start of the test section. The measurements uses hotwire anemometry, set at 20 KHz, measurement period of 10 s, platinum wire of 5 µm, and sensor length of approximately 1.5 mm and overheat ratio of 1.7. The horizontal axis in the plot is the entire extent of test section height i.e. 500 mm. The speed in this measurement is set at approximately 22 m/s or at the highest frequency sent to the controller's VFD. Each measurement point is separated by 10 mm, therefore there are 49 points in this measurement. The solid line indicates mean velocity taken 50 mm from each bottom and top surfaces i.e. four points from each surfaces are omitted from the mean velocity calculation. The dashed-lines indicate 2% deviation from the mean velocities. With all points lie within the 2% deviation, the centerline at 1700 mm is ready for aerodynamic measurement. Note that this is also the location where slot for traverse and infrastructure for rotating table have been allocated.

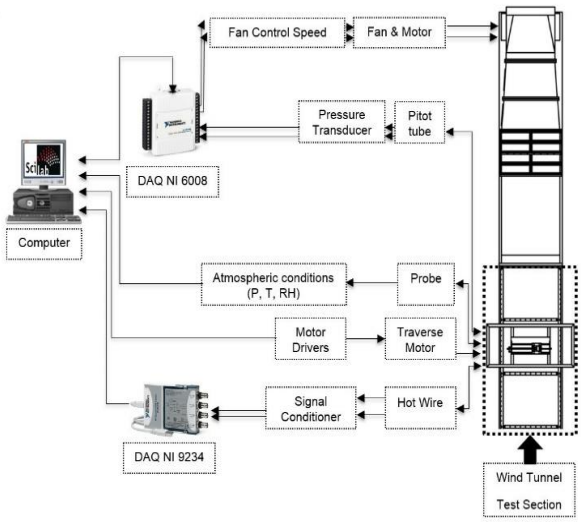

Figure 7 Flow profiles at centerline (y = 0 mm). (a) Velocity profile and (b) Turbulence intensities profile. Where U is the velocity, overbar lines indicate mean values, U_o is the bulk velocity and u' is the fluctuating velocities

Hotwire anemometry calibration has been carried out in-situ. Pitot tube pressure transducer pair has been used to measure flow velocity. Air density and kinematic viscosity have been calculated using the Comet ambience sensor device, therefore the speeds measured in the experiment are considered accurate. Figure 7(b) shows turbulence intensities profile. u', the standard deviation of the fluctuating velocities, scaled with the mean velocity, U_o. The profile suggests that the intensities are relatively large i.e. approximately 5%. The measured turbulence intensities are similar with the ones produced by the Wieghardt's formulation (Eq. 1) as in the results shown in Table 1 and subsequent Batchelor's formulation (Eq. 2). An improvement will have to be done further up in the wind tunnel if lower intensities are required. Currently honeycomb is being installed. From both profiles, the boundary layer thickness δ is approximated to be 50-60 mm i.e. within the expectation from the calculation.

(a) Velocity contour (cross-section) along the middle of the test section

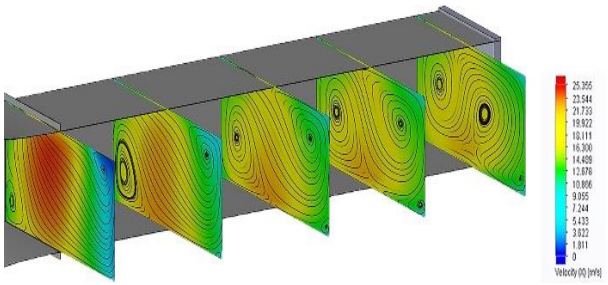

(b) Velocity contour at different location of test section

Figure 8 Velocity flow distribution. (a) Velocity contour profile and (b) velocity contour at a different location. *U* is the velocity

In this section, we describe the flow uniformity by computational fluids dynamic (CFD). The velocity contours of the test section, shown in Figure 8(a), indicates that there is no two-directional flow along the middle section. The flow is from right to left. The flow accelerates towards the end of test section as the boundary layer thickens. Figure 8(b) indicates two low-speed centers which develop on the lower right and upper left of the flow. The centers are being pushed towards each corner as the flow moves towards the end of the test section. The results here are generated without the two layer screen feature. So the actual results which is shown Figure 7(a) might not be readily compared with Figure 8(b). The screens and honeycomb yet to be installed are expected to improve the flow quality.

4.0 CONCLUSION

We have constructed a wind tunnel made mostly from stainless steel body and acrylic body low speed wind tunnel for aerodynamic as well as boundary layer research. Pangkor is capable of 25 m/s speed research and could be run automatically for long period of time. This is possible since all controls are made from one single source - a computer and a software. The internally designed and built wind tunnel allows the turbulence team to go for much focused research. We have omitted computational fluid dynamics (CFD) analysis but only presented selected data for this article.

Acknowledgements

We would like to thank to these organisations for their continued supports in providing various technical assistance,

- *Resolute Engineering Sdn Bhd.* as builder-partner especially for installation of motor-fan and commissioning of VFD,
- *Alam Meridien Sdn. Bhd.* for particle image velocimetry system and some financial contributions,
- *Trity Technologies Sdn.* Bhd. for providing interface with Scilab,
- *Virtual Instrument & System Innovation Sdn.* Bhd. for providing computer-devices interface.

We also like to express our gratitude for financial contributions by these grants:

- FRGS/1/2013/TK01/UKM/03/1 for the constructions of traverse, hotwire accessories and etching apparatus.
- GUP-2013-069 for the installation of three-phase cabling works and installation, temperature sensors, pitot-tubes-pressure transducers.
- *STEM-2014-012 for the timbers, metal supports and paints.*
- *GGPM-2013-93 for the axial fan and motor*
- *AP-2012-010 for the VFD and other accessories*
- *GGPM-2012-092 for the construction of contraction chamber and diffuser sections*
- *FRGS/1/2013/TK01/UKM/02/3 for the installation of sections and fan*
- *PIP-2013-40 for particle image velocimetry (PIV) equipment.*

References

[1] Robins, B. and Curtis, W.S., 1972. *New Principles of Gunnery*. Richmond Publishing Company Limited

[2] Smeaton, J. 1759. An Experimental Enquiry Concerning the Natural Powers of Water and Wind to Turn Mills, and Other Machines, Depending on a Circular Motion. *Philosophical Transactions.* 51: 100-174.

[3] Yakkundi, V., Mantha, S. 2011. *Aerodynamics of Cars: an Experimental Investigation - A Synergy of Wind Tunnel & CFD,* Lambert Academic Publishing.

[4] Marusic, I., Mathis, R. and Hutchins, N. 2010. Predictive Model for Wall-bounded Turbulent Flow. *Science.* 329(5988): 193-196.

[5] Chauhan, K., Hutchins, N., Monty, J. and Marusic, I. 2013. Structure Inclination Angles in the Convective Atmospheric Surface Layer. *Boundary-layer meteorology,* 147(1): 41- 50.

[6] Bailey, A. and Vincent, N.D.G. 1943. Wind-Pressure on Buildings Including Effects of Adjacent Buildings. *Journal of the Institution of Civil Engineers.* 20(8): 243-275.

[7] Cermak, J.E. 2003. Wind-Tunnel Development and Trends in Applications to Civil Engineering. *Journal of Wind Engineering and Industrial Aerodynamics,* 91(3): 355- 370.

[8] Jensen, M. 1958. The Model-Law for Phenomena in Natural Wind, *IngeniNren*. 2(4): 121–128.

[9] Irwin, H.P.A.H. 1981. The Design of Spires for Wind Simulation. *Journal of Wind Engineering and Industrial Aerodynamics.* 7(3): 361-366.

[10] Cook, N.J. 1982. Simulation Techniques for Short Test-Section Wind Tunnels: Roughness, Barrier and Mixing-Device Methods. *Proceedings of the International Workshop on Wind Tunnel Modeling Criteria and Techniques in Civil Engineering Applications.* Gaithersburg, Maryland, Cambridge University Press, London, England. 126-136.

[11] Chan, C.M. and Chui, J.K.L. 2006. Wind-Induced Response and Serviceability Design Optimization of Tall Steel Buildings. *Engineering Structures.* 28(4): 503-513.

[12] Gromke, C. 2011. A Vegetation Modeling Concept for Building and Environmental Aerodynamics Wind Tunnel Tests and Its Application in Pollutant Dispersion Studies. *Environmental Pollution.* 159(8): 2094-2099.
[13] Huang, M.F., Chan, C.M., Lou, W.J. and Kwok, K.C.S. 2012. Statistical Extremes And Peak Factors In Wind-Induced Vibration Of Tall Buildings. *Journal of Zhejiang University SCIENCE A.* 13(1): 18-32.
[14] Tse, K.T., Li, S.W. and Fung, J.C.H. 2014. A Comparative Study of Typhoon Wind Profiles Derived from Field Measurements, Meso-Scale Numerical Simulations, And Wind Tunnel Physical Modeling. *Journal of Wind Engineering and Industrial Aerodynamics.* 131: .46-58.
[15] Harun, Z., Reda, E. and Abdullah, S. 2015. Large Eddy Simulation of the Wind Flow over Skyscrapers. *Recent Advances in Mechanics and Mechanical Engineering.* 15: 72-79.
[16] Noor, A.M. and Mansor, S. 2013. Measuring Aerodynamic Characteristics Using High Performance Low Speed Wind Tunnel at Universiti Teknologi Malaysia. *Journal of Applied Mechanical Engineering.* 3(132): 1-7.
[17] Hasim, F., Rusyadi, R., Surya, W.I., Asrar, W., Omar, A.A., Syed Mohamed Ali, J., Aminanda, Y. and Kafafy, R., 2008. The IIUM Low Speed Wind Tunnel. *2nd Engineering Conference on Sustainable Engineering, Infrastructure Development & Management.* Kuching, Sarawak, Malaysia. 18-19 December 2008.
[18] Reneau, L.R., Johnston, J.P. and Kline, S.J. 1967. Performance and Design of Straight, Two-Dimensional Diffusers. *Journal of Basic Engineering.* 89(1): 41-150.
[19] Lindgren, B. and Johansson, A.V. 2002. *Design and Evaluation of a Low-Speed Wind-Tunnel with Expanding Corners.* Department of Mechanics, KTH, Report No. TRITA-MEK. 14.
[20] Arifuzzaman, M. and Mohammad, M. 2012. Design Construction and Performance Test of a Low Cost Subsonic Wind Tunnel. *IOSR Journal of Engineering.* 10: 83-92.
[21] Gibson, A.H. 1910. On the Flow Of Water Through Pipes and Passages Having Converging or Diverging Boundaries. *Proceedings of the Royal Society of London. Series A, Containing Papers of a Mathematical and Physical Character.* 83(563): 366-378. *Series A, Containing Papers of a Mathematical and Physical Character, 83*(563), 366-378.
[22] Mehta, R.D. and Bradshaw, P. 1979. Design Rules for Small Low-Speed Wind Tunnels. *Aeronautical Journal.* 83(827): 443-449.
[23] Sparrow, E.M., Abraham, J.P. and Minkowycz, W.J. 2009. Flow Separation in A Diverging Conical Duct: Effect of Reynolds Number and Divergence Angle. *International Journal of Heat and Mass Transfer.* 52(13): 3079-3083.
[24] Tulapurkara, E.G. 1980. Studies on Thwaites' Method for Wind Tunnel Contraction. *Aeronautical Journal.* 84: 167-169.
[25] Rouse, H. and Hassan, M.M. 1949. Cavitation-Free Inlets and Contractions. *Mechanical Engineering.* 71(3): 213- 216.
[26] Harun, Z., Abbas, A.A., Etminan, A., Nugroho, B., Kulandaivelu, V. and Khashehchi, M., 2014. Effects of Riblet on Flow Structure around a NACA 0026 Airfoil. In *the 25th International Symposium on Transport Phenomena.*
[27] Harun, Z., 2012. *The Structure of Adverse and Favourable Pressure Gradient Turbulent Boundary Layers.* PhD Thesis. Department of Mechanical Engineering. University of Melbourne.
[28] Mehta, R.D. 1985. Turbulent Boundary Layer Perturbed By a Screen. *AIAA Journal.* 23(9): 1335-1342.
[29] Wieghardt, K.E.G., 1953. On the Resistance of Screens. *Aeronautical Quarterly, 4*(2): 186-192.
[30] Mehta, R.D., 1984, January. Turbulent Flow through Screens. In *AIAA, Aerospace Sciences Meeting* (Vol. 1).
[31]] Mehta, R.D., 2009. *Aspects of the Design of Performance of Blower Tunnel Components.* PhD Thesis. Imperial College, London.
[32] Dryden, H.L. 2012. The Use of Damping Screens for the Reduction of Wind-Tunnel Turbulence. *Journal of the Aeronautical Sciences.* 14(4): 221-228
[33]] Batchelor, G.K. 1953. *The Theory of Homogeneous Turbulence*. Cambridge University Press.
[34] Bell, J.H. and Mehta, R.D., 1988. *Contraction Design for Small Low-Speed Wind Tunnels.* Department of Aeronautics and Astronautics, Stanford University.